
Distributionally Robust Weighted k -Nearest Neighbors

Shixiang Zhu Liyan Xie Minghe Zhang Rui Gao Yao Xie

Abstract

Learning a robust classifier from a few samples remains a key challenge in machine learning. A major thrust of research has been focused on developing k -nearest neighbor (k -NN) based algorithms combined with metric learning that captures similarities between samples. When the samples are limited, robustness is especially crucial to ensure the generalization capability of the classifier. In this paper, we study a minimax distributionally robust formulation of weighted k -nearest neighbors, which aims to find the optimal weighted k -NN classifiers that hedge against feature perturbations. We develop an algorithm, Dr. k -NN, that efficiently solves this functional optimization problem and features in assigning minimax optimal weights to training samples when performing classification. These weights are class-dependent, and are determined by the similarities of sample features under the least favorable scenarios. We also couple our framework with neural-network-based feature embedding. We demonstrate the competitive performance of our algorithm compared to the state-of-the-art in the few-training-sample setting with various real-data experiments.

1. Introduction

Machine learning has been proven successful in data-intensive applications but is often hampered when the data set is small. For example, in breast mammography diagnosis for breast cancer screening (Aresta et al., 2019), the diagnosis of the type of breast cancer requires specialized analysis by pathologists in a highly time- and cost-consuming task and often leads to non-consensual results. As a result, labeled data in digital pathology are generally very scarce; so do many other applications.

In this paper, we aim to tackle the general multi-class classification problem when only very few training samples are available for each class (Wang et al., 2019). Evidently, k -Nearest Neighbor (k -NN) algorithm (Altman, 1992) is a natural idea to tackle this problem and shows promising empirical performances. Notable contributions, including seminal work (Goldberger et al., 2005) and the follow-up

non-linear version (Salakhutdinov & Hinton, 2007), go beyond the vanilla k -NN and propose neighborhood component analysis (NCA). NCA learns a distance metric that optimizes the expected leave-one-out classification error on the training data using a stochastic neighbor selection rule. Some recent studies in few-shot learning also utilize the limited training data using a similar idea, such as matching network (Vinyals et al., 2016), prototypical network (Snell et al., 2017). They are primarily based on distance-weighted k -NN, which classifies an unseen sample (aka. *query*) by a weighted vote of its labeled neighbors and uses the distance between two data points in the embedding space as their weights.

The classification performance of weighted k -NN critically depends on the choice of weighting scheme. In distance-weighted k -NN, the distance measuring the similarity between samples is typically performed by metric learning, where a task-specific distance metric is automatically constructed from supervised data (Koch et al., 2015; Plötz & Roth, 2018; Vinyals et al., 2016). However, it has been recognized that they may be not robust to the *few training samples* scenario, where an “outlier” may greatly deteriorate the performance. An example to illustrate this issue is shown in Figure 1. The training set with only three labeled samples includes two categories we want to classify: mop and Komondor. As we can see, the query is visually closer to the third sample and more likely to be misclassified as a mop with respect to some distance metric, even though it is a Komondor dressing up as a mop. This “outlier” misleads the metric learning model to capture irrelevant details (e.g., the bucket and the mop handle) for the category of Komondor. Such a problem can become even severe when the sample size is small.

The discussion above highlights the importance of choosing a good weighting scheme in weighted k -NN. To develop algorithms that are more robust to the few-training-samples settings, we propose a new formulation of distributionally robust weighted k -nearest neighbors. Given the features of training samples, we solve a Wasserstein distributionally robust optimization problem that finds the minimax optimal weight functions for the k -nearest neighbors. To solve this infinite-dimensional functional optimization problem, we first consider a relaxed problem that solves the distributionally robust multi-classification problem over all randomized



Figure 1. Motivating example: a small training set of three image-label pairs: the first image is a mop; the second image is a dog; the third image looks like a mop but is, in fact, a dog (dressing up as a mop). The query (the last image) is “closer” to the third one and more likely to be misclassified as a dog if we use distance-weighted k -NN.

classifiers (not only restricted to weighted k -NN classifiers). Despite still being infinite-dimensional, this relaxed problem admits a finite-dimensional convex programming reformulation that also outputs the least favorable distributions (LFDs). Next, we show that under such LFDs, there exists a weighted k -NN classifier achieving the same optimal value as the relaxed problem and shares the same LFDs. Thereby we prove the optimality of such weighted k -NN classifier for the original distributionally robust weighted k -nearest neighbors problem. We also discuss the generalization capability of the robust weighted k -NN classifier as compared to the vanilla k -NN.

Based on our theoretical results, we proposed a new algorithm, $\text{Dr. } k\text{-NN}$. Unlike the traditional distance-weighted k -NN that uses the same weight for all label classes, our algorithm introduces a vector of weights, one for each class, for each sample in k -NN and perform a weighted majority vote. These weights are determined from the least favorable distributions on the training samples, which reveal the significance of each sample in the worst case, thereby contributing effectively to final decision making. An example is illustrated in Figure 2.

Further, using differentiable optimization (Agrawal et al., 2019; Amos & Kolter, 2017), we incorporate a neural network into the minimax classifier that jointly learns the feature embedding and the minimax optimal classifier. Numerical experiments show that our algorithm can effectively improve the multi-class classification performance with few training samples on various data sets.

Related work Recently, there has been much interest in the multi-class classification problem with few training samples, see (Wang et al., 2019) for a recent survey. The main idea of our work is related to metric learning (Goldberger et al., 2005; Plötz & Roth, 2018; Salakhutdinov & Hinton, 2007), which essentially translates the hidden information carried by the limited data into a distance metric and has been widely adopted in few-shot learning, meta learning, and other related machine learning problems (Finn et al., 2017; Koch et al., 2015; Li et al., 2006; Snell et al., 2017; Vinyals et al., 2016). However, unlike few-shot learning and

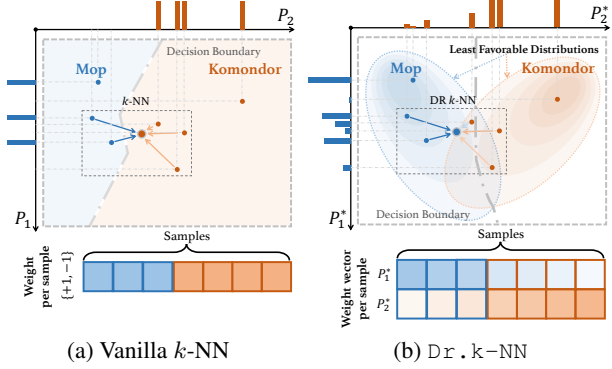


Figure 2. An illustration shows the difference between $\text{Dr. } k\text{-NN}$ and vanilla k -NN. Each colored dot is a training sample, where the color indicates its class-membership. The horizontal/vertical bar represents the probability mass of one training sample under the distribution P_1, P_2 , respectively.

meta learning, where the goal is to acquire meta knowledge from a large number of observed classes and then predicting examples from unobserved classes, we focus on attacking a specific general classification problem where the number of categories is limited but labeled data are difficult to obtain. In this paper, we take a different probabilistic approach to exploit information from the data: differing from the metric learning, we construct an uncertainty set for each class given a distance metric.

Wasserstein distributionally robust optimization (Abadeh et al., 2015; Blanchet & Murthy, 2019; Blanchet et al., 2019; Esfahani & Kuhn, 2018; Gao & Kleywegt, 2016; Gao et al., 2017; Shafieezadeh-Abadeh et al., 2019; Sinha et al., 2017) is an emerging paradigm for statistical learning; see (Kuhn et al., 2019) for a recent survey. Our work is mostly related to (Gao et al., 2018), a framework for Wasserstein robust hypothesis testing, but is different in several important ways. First, we focus on k -NN classifiers for multi-class classification, while (Gao et al., 2018) studied two hypotheses. Second, we focus on directly minimizing the mis-classification error while (Gao et al., 2018) introduces a convex relaxation for the 0-1 loss. Third, while (Gao et al., 2018) requires sample features as an input, we develop a scalable algorithmic framework to simultaneously learn the optimal feature extractor parameterized by neural networks and robust classifier to achieve the best performance. A recent work (Chen & Paschalidis, 2019) studies distributionally robust k -NN regression. Note that regression and classification are fundamentally different as different performance metrics are used: in (Chen & Paschalidis, 2019) the objective is to minimize the mean square error, whereas in our work the performance metric is classification errors. Another well-known work on optimal weighted nearest neighbor binary classifier (Samworth et al., 2012) assigns one weight to each sample; the optimal weights minimize asymptotic expansion for the excess risk (regret). In contrast, we consider minimax robust

multi-class classification, each training sample is associated with different weights for different classes.

2. Distributionally Robust k -NN

In this section, we present our model. We define weighted k -NN classifier in Section 2.1, and present the proposed framework of distributionally robust k -NN problem in Section 2.2.

2.1. Weighted k -NN classifier

Let $\{(x^1, y^1), \dots, (x^n, y^n)\}$ be a set of training samples, where x^i denotes the i -th data sample in the observation space \mathcal{X} , and $y^i \in \mathcal{Y} := \{1, \dots, M\}$ denotes the class (label) of the i -th data sample. Let $\phi : \mathcal{X} \rightarrow \Xi$ be a feature extractor that embeds samples to the feature space Ξ (in Section 4.2 we will train a neural network to learn ϕ). Denote the sample features and the empirical support as

$$\xi^i := \phi(x^i), i = 1, \dots, n, \quad \widehat{\Xi} := \{\xi^1, \dots, \xi^n\}.$$

Let

$$S = \{(\xi^1, y^1), \dots, (\xi^n, y^n)\}.$$

Define empirical distributions

$$\widehat{P}_m := \frac{1}{|\{i : y^i = m\}|} \sum_{i=1}^n \delta_{\xi^i} \mathbb{I}\{y^i = m\}, \quad m = 1, \dots, M,$$

where δ denotes the Dirac point mass, $|\cdot|$ denotes the cardinality of a set, and \mathbb{I} denotes the indicator function.

Let $\pi : \Xi \rightarrow \Delta_M$ be a *randomized* classifier that assigns class $m \in \{1, \dots, M\}$ with probability $\pi_m(\xi)$ to a query feature $\xi \in \Xi$, where Δ_M is the probabilistic simplex $\Delta_M = \{\pi \in \mathbb{R}_+^M : \sum_{m=1}^M \pi_m = 1\}$. It is worth mentioning that the randomized test is more general than the commonly seen deterministic test. In particular, the random classifier π reduces to the deterministic test if for any ξ , there exists a m such that $\pi_m(\xi) = 1$. Suppose the features in each class m follows a distribution P_m . We define the *risk* of a classifier π as the total error probabilities¹

$$\Psi(\pi; P_1, \dots, P_M) := \sum_{m=1}^M \mathbb{E}_{\xi \sim P_m} [1 - \pi_m(\xi)]. \quad (1)$$

Recall that the vanilla k -NN is performed as follows. Let $c : \Xi \times \Xi \rightarrow \mathbb{R}_+$ be a metric on Ξ that measures distance between features. For any given query point ξ , let $\tau_1^S(\xi), \dots, \tau_n^S(\xi)$ be a reordering of $\{1, \dots, n\}$ according to their distance to ξ , i.e., $c(\xi, \xi^{\tau_i^S(\xi)}) \leq c(\xi, \xi^{\tau_{i+1}^S(\xi)})$ for all $i < n$, where the tie is broken arbitrarily. Here the superscript S indicates the dependence on the sample S . We

¹To ease the exposition we consider only equal weights over the error probabilities, but our results can be easily generalized to any weighted average of error probabilities.

compute the votes as

$$p_m(\xi) := \sum_{i=1}^k \frac{1}{k} \mathbb{I}\{y^{\tau_i^S(\xi)} = m\}, \quad m = 1, \dots, M. \quad (2)$$

The vanilla k -NN decides the class for ξ by the majority vote, i.e., accept the class $\arg \max_{1 \leq m \leq M} p_m(\xi)$.

To define a weighted k -NN, let us replace the equal weights in (2) by an arbitrary weight function $w_m : \Xi \times \Xi \rightarrow \mathbb{R}_+$ for each class $m = 1, \dots, M$:

$$p_m(\xi) := \sum_{i=1}^k w_m(\xi, \xi^{\tau_i^S(\xi)}), \quad (3)$$

and use a shorthand notation $w := (w_1, \dots, w_M)$. In the sequel, we define a general tie-breaking rule as follows. For any ξ , denote $\mathcal{M}_0(\xi) := \arg \max_{1 \leq m \leq M} p_m(\xi)$. When $|\mathcal{M}_0(\xi)| > 1$, there is a tie at ξ . We denote $\pi_m(\xi)$ as the probability of accepting class m for $m \in \mathcal{M}_0(\xi)$ and we have $\sum_{m \in \mathcal{M}_0(\xi)} \pi_m(\xi) = 1$.

We define a *weighted k -NN classifier* $\pi^{\text{knn}}(\xi; k, w) : \Xi \rightarrow \Delta_M$ as

$$\pi_m^{\text{knn}}(\xi; k, w) = \begin{cases} \pi_m(\xi), & m \in \mathcal{M}_0(\xi), \\ 0, & \text{otherwise.} \end{cases} \quad (4)$$

A weighted k -NN classifier involves two parameters: number of nearest neighbors k and weighting scheme w . Particularly, $w_m(\xi, \xi^i) = \mathbb{I}\{y^i = m\}$ recovers the vanilla k -NN, and $w_m(\xi, \xi^i) = \mathbb{I}\{y^i = m\}/c(\xi, \xi^i)$ recovers the distance-based weighted k -NN. Note that our definition (3) allows different weighting schemes for different classes, which is more general than the standard weighted k -NN.

The goal is to find the optimal weighted k -NN classifier $\pi^{\text{knn}}(\cdot; k, w)$ such that the risk Ψ as defined in (1) is minimized. Since the underlying true distributions of the samples are unknown, the commonly used loss function is the empirical loss, i.e., substitute the empirical distributions \widehat{P}_m into the risk function (1). This leads to the following optimization problem

$$\min_{\substack{1 \leq k \leq n \\ w_m : \Xi \times \Xi \rightarrow \mathbb{R}_+, 1 \leq m \leq M}} \Psi(\pi^{\text{knn}}(\cdot; k, w); \widehat{P}_1, \dots, \widehat{P}_M). \quad (5)$$

It is worth mentioning that this minimization problem is an *infinite-dimensional* functional optimization, since the weighting schemes w is a function on $\Xi \times \Xi$.

2.2. Distributionally robust k -NN

For few-training-sample setting, the empirical distributions might not be good estimates for the true distribution since the sample size is small. To hedge against distributional uncertainty, we propose a distributionally robust counterpart of the weighted k -NN problem defined in the previous

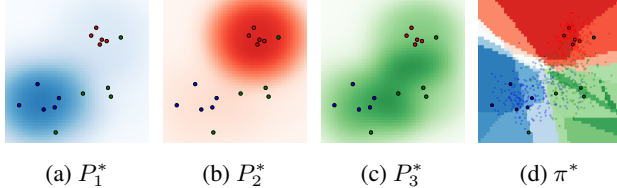

 (a) P_1^* (b) P_2^* (c) P_3^* (d) π^*

Figure 3. An example of the weights P_1^*, P_2^*, P_3^* yielding from (9) and the corresponding results of $\text{Dr. } k\text{-NN}$ using a small subset of MNIST (digit 4 (red), 6 (blue), 9 (green) and $k = 5$). Raw samples are projected on a 2D feature space ($d = 2$), with the color indicating their true class-membership. In (a)(b)(c), shaded areas indicate the kernel smoothing of P_1^*, P_2^*, P_3^* defined in (12). In (d), big dots represent the training points and small dots represent the query points, and their color depth suggests how likely the sample is being classified into the true category.

subsection. Specifically, suppose each class m is associated with a distributional uncertainty set \mathcal{P}_m , which will be specified shortly. Given $\mathcal{P}_1, \dots, \mathcal{P}_M$, define the *worst-case risk* of a classifier π as the worst-case total error probabilities

$$\max_{P_m \in \mathcal{P}_m, 1 \leq m \leq M} \Psi(\pi; P_1, \dots, P_M),$$

where Ψ is defined in (1).

We consider the following distributionally robust k -NN problem that finds the optimal weighted k -NN classifier minimizing the worst-case risk:

$$\min_{\substack{1 \leq k \leq n \\ w_m: \Xi \times \Xi \rightarrow \mathbb{R}_+ \\ 1 \leq m \leq M}} \max_{P_m \in \mathcal{P}_m} \Psi(\pi^{\text{knn}}(\cdot; k, w); P_1, \dots, P_M). \quad (6)$$

Here the optimal solution P_1^*, \dots, P_M^* to the inner maximization problem is also called *least favorable distributions (LFD)* in statistics literature (Huber, 1965).

Now let us describe the uncertainty set \mathcal{P}_m . First, since we are going to re-weight the training samples to build the classifier, we will restrict the support of every distribution in \mathcal{P}_m to $\widehat{\Xi}$, the set of empirical points. Second, the uncertainty set is data-driven, containing the empirical distribution \widehat{P}_m and distributions surrounding its neighborhood. Third, to measure the closeness between distributions, we would like to choose the Wasserstein metric of order 1 (Villani, 2008), defined as

$$\mathcal{W}(P, P') := \min_{\gamma} \mathbb{E}_{(\xi, \xi') \sim \gamma} [c(\xi, \xi')]$$

for any two distributions P and P' on Ξ , where the minimization of γ is taken over the set of all probability distributions on $\Xi \times \Xi$ with marginals P and P' . The main advantage of using Wasserstein metric is that it takes account of the *geometry* of the feature space by incorporating the metric $c(\cdot, \cdot)$ in its definition. Given the empirical distribution \widehat{P}_m for $m = 1, \dots, M$, we define

$$\mathcal{P}_m := \{P_m \in \mathcal{P}(\widehat{\Xi}) : \mathcal{W}(P_m, \widehat{P}_m) \leq \vartheta_m\}, \quad (7)$$

where $\mathcal{P}(\widehat{\Xi})$ denotes the set of all probability distributions on $\widehat{\Xi}$; $\vartheta_m \geq 0$ specifies the size of the uncertainty set for the m -th class that specifies the amount of deviation we would like to control.

3. Theoretical Properties

In this section, we analyze the computational tractability and statistical properties of the proposed distributionally robust weighted k -NN classifier. All proofs are delegated to Section A in the supplementary material.

Observe that similar to (5), the formulation (6) is also an infinite-dimensional functional optimization. Let us first relate it to a (infinite-dimensional) relaxed robust classification problem, which turns out to be more tractable. The following result is on the expressive power of the class of weighted k -NN classifiers

$$\{\pi^{\text{knn}}(\xi; k, w)\}_{w_m: \Xi \times \Xi \rightarrow \mathbb{R}_+, 1 \leq m \leq M}$$

defined in Section 2.1. Consider the following minimax robust classification problem over all randomized classifiers π (recalling Δ_M is the probability simplex in \mathbb{R}_+^M):

$$\min_{\pi: \Xi \rightarrow \Delta_M} \max_{P_m \in \mathcal{P}_m, 1 \leq m \leq M} \Psi(\pi; P_1, \dots, P_M). \quad (8)$$

Yet still, (8) is an infinite-dimensional functional optimization, since we are optimizing over the set of all randomized classifiers. We establish the following theorem stating a finite-dimensional convex programming reformulation for the problem (8).

Theorem 1. *For the uncertainty sets defined in (7), the least favorable distribution of problem (8) can be obtained by solving the following problem:*

$$\begin{aligned} & \min_{\substack{p_1, \dots, p_M \in \mathbb{R}_+^n \\ \gamma_1, \dots, \gamma_M \in \mathbb{R}_+^{n \times n}}} \sum_{i=1}^n \max_{1 \leq m \leq M} p_m^i \\ & \text{subject to} \quad \sum_{i=1}^n \sum_{j=1}^n \gamma_m^{i,j} c(\xi^i, \xi^j) \leq \vartheta_m, \\ & \quad \sum_{i=1}^n \gamma_m^{i,j} = \widehat{P}_m(\xi^j), \quad \sum_{j=1}^n \gamma_m^{i,j} = p_m^i, \\ & \quad \forall 1 \leq i, j \leq N, 1 \leq m \leq M. \end{aligned} \quad (9)$$

The decision variable $\gamma_m \in \mathbb{R}_+^{n \times n}$ can be viewed as a joint distribution on n empirical points with marginal distributions \widehat{P}_m and P_m , represented by a vector $p_m \in \mathbb{R}_+^n$. The inequality constraint controls the Wasserstein distance between P_m and \widehat{P}_m . Let $y_m^i \in \{0, 1\}$ be the class indicator variable of sample ξ^i . The objective in (9) can be equiva-

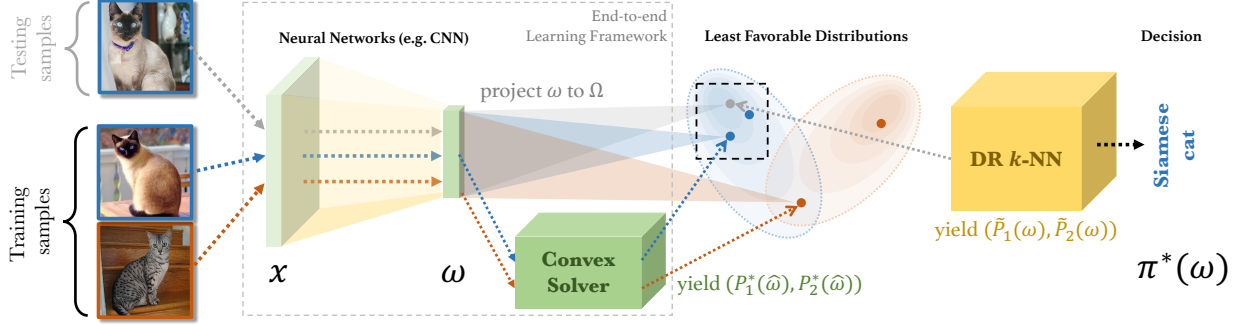


Figure 4. An overview of the end-to-end learning framework, which consists of two cohesive components: (1) an architecture that is able to produce feature embedding ξ and least favorable distributions P_m^* for training set; (2) an DR . k -NN makes decisions for any unseen sample ξ based on the estimated weight vector $\tilde{p}_m(\xi)$ (probability mass on least favorable distributions).

lently rewritten as minimization of total margin

$$\sum_{i=1}^n \sum_{m=1}^M \left(\max_{1 \leq m' \leq M} p_{m'}^i - p_m^i \right),$$

where $\max_{1 \leq m' \leq M} p_{m'}^i - p_m^i$ measures the margin between the maximum likelihood of ξ^i among all classes and the likelihood of the m -th class of ξ^i . When $M = 2$, the total margin reduces to the total variation distance. Also, observe that

$$\begin{aligned} \sum_{i=1}^n \max_{1 \leq m \leq M} p_m^i &= \lim_{t \rightarrow \infty} \left(\sum_{i=1}^n \sum_{m=1}^M y_m^i p_m^i - \right. \\ &\quad \left. \frac{1}{t} \sum_{i=1}^n \sum_{m=1}^M y_m^i \log \frac{\exp(tp_m^i)}{\sum_{m=1}^M \exp(tp_m^i)} \right), \end{aligned}$$

where the second term on the right side represents the cross-entropy (or negative log-likelihood). Therefore, problem (9) perturbs $(\hat{P}_1, \dots, \hat{P}_M)$ to LFDs (P_1^*, \dots, P_M^*) so as to minimize the total margin as well as an upper bound on cross-entropy of LFDs; the smaller the margin (or cross-entropy) is, the more similar between classes and thus the harder to distinguish among them.

The following theorem establishes the equivalence between the original problem (6) and the relaxed problem (8).

Theorem 2. *For the uncertainty set defined in (7), formulations (8) and (6) have identical optimal values. In addition, there exists optimal solutions of (8) and (6) that share common LFDs that are optimal to (9).*

Theorem 2 implies that the set of weighted k -NN classifiers is exhaustive, in the sense that it achieves the same optimal robust risk as optimizing over the set of all randomized classifiers. In our proof, we show that the weighted 1-NN classifier, with weights equal to the LFDs of (9), is an optimal solution to (6). Therefore, instead of solving (6) directly, by Theorem 1, we can solve the convex program (9) for the LFDs, based on which we construct a robust

k -NN classifier. This justifies the DR . k -NN algorithm to be described in the next section.

Next, we discuss the out-of-sample performance – measured by the population risk under the true distribution – of the proposed distributional robust k -NN framework. Given a training set $S = \{(\xi^i, y^i)\}_{i=1}^n$, let \mathcal{D} be the distribution on $\Xi \times \mathcal{Y}$ from which S is sampled. Let \mathcal{D}_Ξ be the marginal distribution of feature vectors ξ and $\eta : \Xi \rightarrow \Delta_M$ be the conditional probability over the labels, i.e., $\eta_m(\xi) = \mathbb{P}[y = m | \xi]$. Note that in such setting, the Bayes optimal test, which accepts the class with the largest conditional probability, is optimal in terms of minimizing the true population risk. Let $\pi^S : \widehat{\Xi} \rightarrow \Delta_M$ be the optimal k -NN classifier corresponding to the LFDs to (6), i.e., π^S and (P_1^*, \dots, P_M^*) are the solution to the saddle point problem (8). Then optimal robust k -NN classifier classifies a sample $\xi \in \Xi$ into class m with probability $\pi_m^S(\xi) = \pi_m^S(\xi^{\tau_1^S(\xi)})$.

For radius small enough such that there is a unique maximum among the LFDs on the nearest neighbor $\xi^{\tau_1^S(\xi)}$ (i.e., there is no tie), the optimal robust 1-NN classifier will reduce to the vanilla 1-NN classifier since the unique maximum will be obtained at the class of $\xi^{\tau_1^S(\xi)}$ (e.g., consider the simplest case $\vartheta_m = 0$). When the radius is selected moderately large such that there is a tie, the optimal robust 1-NN classifier might achieve better performance than vanilla 1-NN. More specifically, we assume that given samples S and a query feature ξ , there is a tie at $\xi^{\tau_1^S(\xi)}$ between classes $m_1^S, \dots, m_{K_S}^S$ for some $K_S \leq M$, thus we have $\pi_m^S(\xi^{\tau_1^S(\xi)}) = 0$ for $m \notin \{m_1^S, \dots, m_{K_S}^S\}$. We have the following results.

Theorem 3. *The population risk under the true distribution of the distributionally robust 1-NN classifier is*

$$\mathbb{E}_{S \sim \mathcal{D}^n, \xi \sim \mathcal{D}_\Xi} \left[\sum_{k=1}^{K_S} \pi_{m_k^S}^S(\xi) \cdot (1 - \eta_{m_k^S}(\xi)) \right],$$

which can be decomposed into the risk of vanilla 1-NN and

a residual term

$$\mathbb{E}_{S,\xi} \left[\sum_{m=1}^M \left(\eta_m(\xi) - \sum_{k=1}^{K_S} \pi_{m_k^S}^S(\xi) \eta_{m_k^S}(\xi) \right) \cdot \eta_m(\xi^{\tau_1^S(\xi)}) \right]. \quad (10)$$

Note that for any $\xi \in \Xi$, the mis-classification probability of optimal robust 1-NN is smaller than vanilla 1-NN if the quantity inside the expectation in (10) is negative; this condition can be viewed as the weighted average over $\eta_m(\xi) - \sum_{k=1}^{K_S} \pi_{m_k^S}^S(\xi) \eta_{m_k^S}(\xi)$. In other words, the risk is controlled by the accepting probabilities π^S .

By the definition of Wasserstein distance, it is more likely to have a tie when some empirical samples from different classes are close in metric $c(\cdot, \cdot)$ (those points may lead to mis-classification results). For example, when ξ and $\xi^{\tau_1^S(\xi)}$ are located in *opposite* sides *near* the true Bayes decision boundaries: $\exists m$ such that $\eta_m(\xi^{\tau_1^S(\xi)})$ is the largest conditional probability and $\exists m'$ such that $\eta_{m'}(\xi)$ is the largest conditional probability for ξ . In such cases, the quantity inside the expectation (10) can be negative when $\pi_{m'}^S$ is set large enough, and the optimal robust 1-NN outperforms vanilla 1-NN, which accepts the “wrong” class m with high probability. Such advantage will exist more often in the few-sample-size regime (see e.g., Figure 2, where the query is indeed close to a training sample from a different class).

4. Proposed Algorithm Dr . k-NN

In this section, we present the Distributional robust k -Nearest Neighbor (Dr . k-NN) algorithm, which is a direct consequence of the theoretical justifications in Section 3.

4.1. Dr . k-NN algorithm

Based on Theorem 2, our algorithm contains two steps.

Step 1. [Sample re-weighting] For each class m , re-weight n samples using a distribution P_m^* , where (P_1^*, \dots, P_M^*) is the p -component of the minimizer of the convex program (9).

Step 2. [k-NN] Given a query point ξ , ordering the training samples according to their distance to ξ : $c(\xi, \xi^{\tau_1^S(\xi)}) \leq c(\xi, \xi^{\tau_2^S(\xi)}) \leq \dots \leq c(\xi, \xi^{\tau_n^S(\xi)})$. Compute the weighted k -NN votes, define

$$\tilde{p}_m(\xi) := \frac{1}{k} \sum_{i=1}^k P_m^*(\xi^{\tau_i^S(\xi)}), \quad m = 1, \dots, M. \quad (11)$$

Decide the class for a query feature point ξ as $\arg \max_{1 \leq m \leq M} \tilde{p}_m(\xi)$, where the tie is broken according to the rule (4).

Figure 3 gives an illustration showing the probabilistic weights (P_1^*, P_2^*, P_3^*) for three classes and its corresponding decision boundary yielding from the weighted k -NN.

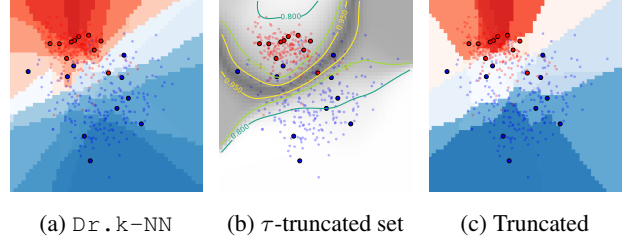


Figure 5. An example of the truncated Dr . k-NN using MNIST (digit 4 (red) and 9 (blue)). Big dots represent training samples and small dots represent query samples. (a) shows the decision made by Dr . k-NN; (c) shows the decision made by the truncated Dr . k-NN with truncation level $\tau = 0.9$; (b) shows τ -truncated regions with $\tau = 0.95, 0.9, 0.8$. Big dots between the lines are selected training samples under different τ . The depth of the shaded area shows the level of samples entropy.

For the sake of completeness, we also extend our algorithm to non-few-training-sample setting, which is referred to as truncated Dr . k-NN, as shown in Figure 5. The key idea is to keep the training samples that are important in deciding the decision boundary based on the maximum entropy principle (Cover & Thomas, 2006). This can be particularly useful for the general classification problem with an arbitrary size of training set. Details can be found in Section B of the supplementary material.

4.2. Jointly learning framework

In this section, we propose a framework that jointly learns the feature mapping and the robust classifier. Let the feature mapping $\phi(\cdot; \theta)$ be a neural network parameterized by θ whose input is a batch of training samples (Figure 4), and then compose it with an optimization layer that packs the convex problem (9) as an output layer that outputs the LFDs of (8). The optimization layer is adopted from differentiable optimization (Agrawal et al., 2019; Amos & Kolter, 2017), in which the optimization problem is integrated as an individual layer in an end-to-end trainable deep networks and the solution of the problem can be backpropagated through neural networks.

To apply the mini-batch stochastic gradient descent, we need to ensure that each batch comprises of multiple “mini-sets”, one for each class, containing at least one training sample from each class fed into the convex optimization layer.

In light of (9), the objective of our joint learning framework is $\min_{\theta} J(\theta; P_1^*, \dots, P_M^*)$, where

$$J(\theta; P_1^*, \dots, P_M^*) := \sum_{i=1}^n \max_{1 \leq m \leq M} P_m^*(\phi(x^i; \theta)),$$

and $\{P_m^*(\phi(\cdot; \theta))\}_{1 \leq m \leq M}$ are the LFDs generated by the convex solver defined in (9) given input variables $\{\xi^i = \phi(x^i; \theta)\}_{1 \leq i \leq n}$. The algorithm is summarized in Algorithm 1.

Algorithm 1 Learning algorithm for $\text{Dr. } k\text{-NN}$

Input: $S_m := \{(x^i, y^i) : y^i = m, \forall i\} \subset S, m = 1, \dots, M$;

Output: The feature mapping $\phi(\cdot; \theta)$ and the LFD P_1^*, \dots, P_M^* supported on training samples;

Initialization: θ_0 is randomly initialized; $n' < n$ is the size of “mini-set”; $t = 0$;

while $t < T$ **do**

- for** number of mini-sets **do**

 - Randomly generate M integers n_1, \dots, n_M such that $\sum_{m=1}^M n_m = n'$; $n_m > 0, \forall m$;
 - Initialize two ordered sets $\widehat{\Xi} = \emptyset, \widehat{P} = \emptyset$
 - for** $m \in \{1, \dots, M\}$ **do**

 - $\mathcal{X}_m \leftarrow$ Randomly sample n_m points from S_m ;
 - $\widehat{\Xi}_m \leftarrow \{\xi := \phi(x; \theta_t) : x \in \mathcal{X}_m\}$;
 - $\widehat{P}_m \leftarrow \frac{1}{n_m} \sum_{i=1}^{n_m} \delta_{\xi_m^i}, \xi_m^i \in \widehat{\Xi}_m$;
 - $\widehat{\Xi} \leftarrow \widehat{\Xi} \cup \widehat{\Xi}_m; \widehat{P} \leftarrow \widehat{P} \cup \widehat{P}_m$;

 - end**
 - Update the probability mass of LFDs P_1^*, \dots, P_M^* on $\widehat{\Xi}$ by solving (9) given $\widehat{\Xi}, \widehat{P}$;

- end**
- $\theta_{t+1} \leftarrow \theta_t - \alpha \nabla J(\theta_t; P_1^*, \dots, P_M^*)$, where α is the learning rate; $t \leftarrow t + 1$;

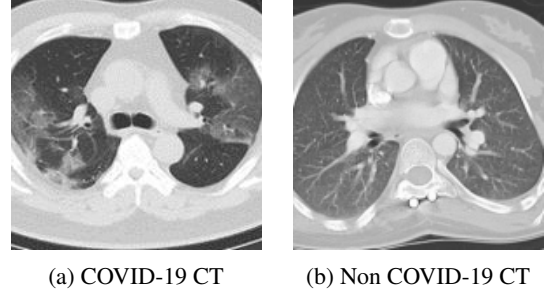
end

In this section, we evaluate our method and eight alternative approaches on four commonly-used image data sets: MNIST (LeCun & Cortes, 2010), CIFAR-10 (Krizhevsky et al., 2020), Omniglot (Lake et al., 2015), and present a set of comprehensive numerical examples. We also test our method on two medical diagnosis data sets: Lung Cancer (Dua & Graff, 2017), and COVID-19 CT (Yang et al., 2020), where very few data samples are available for study, due to privacy concerns and high costs associated with harvesting data. Specifically, Lung Cancer data record 56 attributes for only 32 patients who have been diagnosed with three types of pathological lung cancers; COVID-19 Computed Tomography (CT) data contain 349 COVID-19 CT images from 216 patients and 463 non-COVID-19 CTs. Here, we present a pair of COVID-19 CT image and non-COVID-19 CT image in Figure 6. More examples can be found in Section D of the supplementary material.

5. Experiments

5.1. Experiment set-up

We compare our method including $\text{Dr. } k\text{-NN}$ and its truncated version with the following baselines: (1) k -NN based methods with different dimension reduction techniques, including Principal Component Analysis (PCA+ k -NN), Singular Value Decomposition (SVD+ k -NN), Neighbourhood



(a) COVID-19 CT

(b) Non COVID-19 CT

Figure 6. An example of the comparison between a COVID-19 CT image and a non-COVID-19 CT image.

Components Analysis (NCA+ k -NN) (Goldberger et al., 2005), and feature embeddings generated by Dr. k -NN (Feature embedding + k -NN) as a sanity check; (2) matching networks (Vinyals et al., 2016); (3) prototypical networks (Snell et al., 2017); (4) MetaOptNet (Lee et al., 2019). To make these methods comparable, we adopt the same naive neural network with a single CNN layer on matching network, prototypical network, and our model, respectively, where the kernel size is 3, the stride is 1 and the width of the output layer is $d = 400$.

In our experiments, we focus on an M -class K -sample (K training samples for each class) learning task. To generate the training data set, we randomly select M classes and for each class we take K random samples. So our training data set contains MK samples overall. We then aim to classify a disjoint batch of unseen samples into one of these M classes. Thus random performance on this task stands at $1/M$. We test the average performance of different methods using 1,000 unseen samples from the same M classes. To obtain reliable results, we repeat each test 10 times and calculate the average accuracy.

Other experimental configurations are described as follows: The Adam optimizer (Kingma & Ba, 2014) is adopted for all experiments conducted in this paper, where learning rate is 10^{-2} . The mini-batch size is 32. The hyper-parameter ϑ_m is chosen by cross-validation, which varies from application to application. The differentiable convex optimization layer we adopt is from (Agrawal et al., 2019). To make all approaches comparable, we use the same network structure in matching network, prototypical network, and MetaOptNet as we described above. We use the Euclidean distance $c(\xi, \xi') = \|\xi - \xi'\|_2$ throughout our experiment.

5.2. Results

We present the average test accuracy in Table 1 for the unseen samples with different $M = 2, 5$ and $K = 5, 10$ on small subsets of MNIST, *mini* ImageNet, CIFAR-10, Omniglot, and with $M = 3$ and $K = 5, 8$ on lung cancer data. Note that random performance for two-class and five-class classifications are 0.5 and 0.2, respectively. The figures in Table 1 show that $\text{Dr. } k\text{-NN}$ ($k = 5$) outperforms other

Table 1. Comparison of classification accuracy in the few-training-sample setting

Methods	MNIST				mini ImageNet				CIFAR-10				Omniglot				Lung Cancer			COVID-19 CT	
	$M = 2$ $K = 5$	$M = 2$ $K = 10$	$M = 5$ $K = 5$	$M = 5$ $K = 10$	$M = 2$ $K = 5$	$M = 2$ $K = 10$	$M = 5$ $K = 5$	$M = 5$ $K = 10$	$M = 2$ $K = 5$	$M = 2$ $K = 10$	$M = 5$ $K = 5$	$M = 5$ $K = 10$	$M = 2$ $K = 5$	$M = 2$ $K = 10$	$M = 5$ $K = 5$	$M = 5$ $K = 10$	$M = 3$ $K = 5$	$M = 3$ $K = 8$	$M = 2$ $K = 5$	$M = 2$ $K = 10$	
PCA+ k -NN	0.801	0.872	0.614	0.678	0.578	0.667	0.268	0.277	0.687	0.711	0.262	0.270	0.597	0.638	0.309	0.358	0.617	0.647	0.658	0.719	
SVD+ k -NN	0.749	0.790	0.524	0.567	0.587	0.675	0.268	0.283	0.680	0.701	0.259	0.266	0.591	0.618	0.305	0.413	0.624	0.648	0.646	0.715	
NCA+ k -NN	0.602	0.640	0.340	0.355	0.547	0.578	0.245	0.258	0.597	0.616	0.232	0.236	0.549	0.574	0.267	0.346	0.575	0.582	0.612	0.624	
Matching Net	0.732	0.830	0.625	0.732	0.687	0.703	0.286	0.360	0.632	0.641	0.241	0.247	0.735	0.769	0.412	0.433	0.621	0.635	0.715	0.732	
Prototypical Net	0.742	0.842	0.671	0.759	0.710	0.725	0.296	0.348	0.651	0.664	0.254	0.259	0.769	0.836	0.448	0.532	0.632	0.644	0.729	0.744	
MetaOptNet	0.725	0.843	0.658	0.790	0.732	0.741	0.255	0.363	0.702	0.713	0.257	0.298	0.742	0.755	0.412	0.453	0.638	0.642	0.713	0.739	
Feature embedding + k -NN	0.792	0.798	0.546	0.551	0.738	0.742	0.490	0.486	0.689	0.691	0.492	0.494	0.725	0.751	0.445	0.495	0.664	0.691	0.701	0.710	
Kernel Smoothing	0.777	0.873	0.559	0.579	0.593	0.601	0.272	0.278	0.642	0.661	0.272	0.282	0.520	0.565	0.240	0.285	0.367	0.370	0.582	0.604	
Truncated Drk-NN	0.815	0.926	0.742	0.825	0.746	0.753	0.295	0.340	0.703	0.719	0.297	0.305	0.755	0.825	0.425	0.542	0.652	0.693	0.722	0.741	
Dr-k-NN	0.838	0.959	0.746	0.831	0.752	0.786	0.306	0.358	0.707	0.728	0.309	0.311	0.765	0.850	0.465	0.580	0.667	0.704	0.734	0.752	

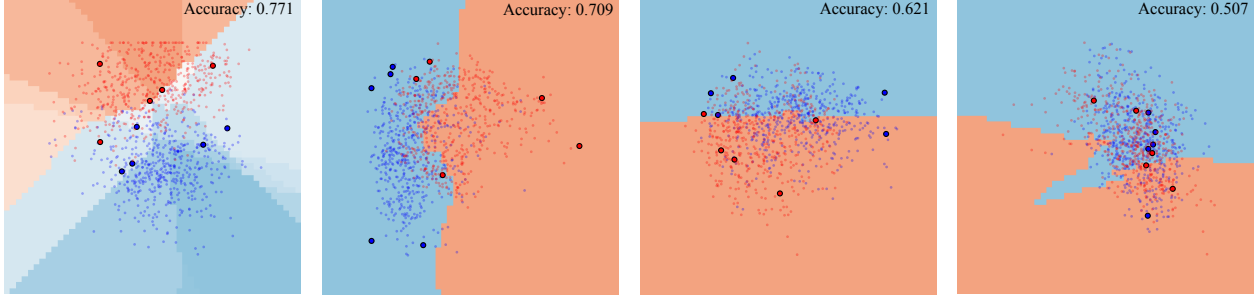


Figure 7. A comparison of the learned feature spaces and the corresponding decision boundaries. There are 10 training samples from two categories of MNIST identified as large dots and 1,000 query samples identified as small dots. The color of dots shows their true categories. The color of the region shows the decisions made by corresponding methods.

baselines in terms of the average test accuracy on all data sets. The truncated Dr. k -NN also yields competitive results using only 20% training samples ($\tau = 0.9$), compared to standard Dr. k -NN.

To confirm that the proposed learning framework will affect the distribution of hidden representation of data points, we show the training and query samples in a 2D feature space and the corresponding decision boundary in Figure 7. It turns out our framework finds a better feature representation in the 2D space with a smooth decision boundary and a reasonable decision confidence map (indicated by the color depth in Figure 7 (a)).

5.3. Comparison to kernel smoothing

Here we also compare with an approach using kernel-smoothing of the LFDs (in contrast to using k -NN) for performing classification. Consider a Gaussian kernel $\kappa(x) = |H_h|^{-1/2}\kappa(H_h^{-1/2}x)$, where $H_h = hI_p$ is the isotropical kernel with bandwidth h . Then we replace $\tilde{p}_m(\xi)$ in Step 2 of Dr. k -NN with the following

$$\tilde{p}_m(\xi) := \sum_{i=1}^n P_m^*(\xi^i)\kappa(\xi - \xi^i), \quad \forall m, \xi. \quad (12)$$

We evaluate both methods on a subset of MNIST, which contains 1,000 testing samples (small dots) and 20 training samples (large dots) from two categories (indexed by blue and red, respectively). As shown in Figure 8 and Figure 9 (Section C of the supplementary material), our experimental results have shown the importance of using k -NN in our

proposed algorithm, where the Dr. k NN significantly outperforms the parallel version using kernel smoothing (even after the kernel bandwidth being optimized). We find that the performance when using kernel smoothing (12) heavily depends on selecting an appropriate kernel bandwidth h as illustrated by Figure 9. Moreover, the best kernel bandwidth may vary from one dataset to another. Therefore, the cross-validation is required to be carried out to find the best kernel bandwidth in practice, which is quite time-consuming. In contrast, choosing the hyper-parameter k is an easy task, since we only have limited choices of k in few-training-sample scenario and the performance of Dr. k -NN is insensitive to the choices of k (see Figure 8).

6. Conclusion

We propose a distributionally robust k -NN classifier (Dr. k -NN) for tackling the multi-class classification problem with few training samples. To make a decision, each neighboring sample is weighted according to least favorable distributions resulting from a distributionally robust problem. As demonstrated by our experiments, our methods achieve the outstanding performance in accuracy of the classification compared with other baselines using minimal resources. The robust classifier layer (9) serves an alternative to the usual softmax layer in a neural network for classification, and we believe it is promising for other machine learning tasks.

References

Abadeh, S. S., Esfahani, P. M. M., and Kuhn, D. Distributionally robust logistic regression. In *Advances in Neural Information Processing Systems*, pp. 1576–1584, 2015.

Agrawal, A., Amos, B., Barratt, S., Boyd, S., Diamond, S., and Kolter, J. Z. Differentiable convex optimization layers. In *Advances in Neural Information Processing Systems*, pp. 9558–9570, 2019.

Altman, N. S. An introduction to kernel and nearest-neighbor nonparametric regression. *The American Statistician*, 46(3):175–185, 1992. doi: 10.1080/00031305.1992.10475879.

Amos, B. and Kolter, J. Z. Optnet: Differentiable optimization as a layer in neural networks. In *Proceedings of the 34th International Conference on Machine Learning - Volume 70*, pp. 136–145. JMLR. org, 2017.

Aresta, G., Araújo, T., Kwok, S., Chennamsetty, S. S., Safwan, M., Alex, V., Marami, B., Prastawa, M., Chan, M., Donovan, M., Fernandez, G., Zeineh, J., Kohl, M., Walz, C., Ludwig, F., Braunewell, S., Baust, M., Vu, Q. D., To, M. N. N., Kim, E., Kwak, J. T., Galal, S., Sanchez-Freire, V., Brancati, N., Frucci, M., Riccio, D., Wang, Y., Sun, L., Ma, K., Fang, J., Kone, I., Boulmane, L., Campilho, A., Eloy, C., Polónia, A., and Aguiar, P. Bach: Grand challenge on breast cancer histology images. *Medical Image Analysis*, 56:122 – 139, 2019. ISSN 1361-8415. doi: <https://doi.org/10.1016/j.media.2019.05.010>.

Blanchet, J. and Murthy, K. Quantifying distributional model risk via optimal transport. *Mathematics of Operations Research*, 44(2):565–600, 2019.

Blanchet, J., Kang, Y., and Murthy, K. Robust Wasserstein profile inference and applications to machine learning. *Journal of Applied Probability*, 56(3):830–857, 2019.

Chen, R. and Paschalidis, I. Selecting optimal decisions via distributionally robust nearest-neighbor regression. In Wallach, H., Larochelle, H., Beygelzimer, A., d'Alché Buc, F., Fox, E., and Garnett, R. (eds.), *Advances in Neural Information Processing Systems 32*, pp. 749–759. Curran Associates, Inc., 2019.

Cover, T. M. and Thomas, J. A. *Elements of Information Theory (Wiley Series in Telecommunications and Signal Processing)*. Wiley-Interscience, USA, 2006. ISBN 0471241954.

Dua, D. and Graff, C. UCI machine learning repository: Lung cancer data set, 2017.

Esfahani, P. M. and Kuhn, D. Data-driven distributionally robust optimization using the Wasserstein metric: Performance guarantees and tractable reformulations. *Mathematical Programming*, 171(1-2):115–166, 2018.

Finn, C., Abbeel, P., and Levine, S. Model-agnostic meta-learning for fast adaptation of deep networks. In Precup, D. and Teh, Y. W. (eds.), *Proceedings of the 34th International Conference on Machine Learning*, volume 70 of *Proceedings of Machine Learning Research*, pp. 1126–1135, International Convention Centre, Sydney, Australia, 06–11 Aug 2017. PMLR.

Gao, R. and Kleywegt, A. J. Distributionally robust stochastic optimization with Wasserstein distance. *arXiv preprint arXiv:1604.02199*, 2016.

Gao, R., Chen, X., and Kleywegt, A. J. Wasserstein distributional robustness and regularization in statistical learning. *arXiv preprint arXiv:1712.06050*, 2017.

Gao, R., Xie, L., Xie, Y., and Xu, H. Robust hypothesis testing using Wasserstein uncertainty sets. In *Proceedings of the 32nd International Conference on Neural Information Processing Systems, NIPS'18*, pp. 7913–7923, Red Hook, NY, USA, 2018. Curran Associates Inc.

Goldberger, J., Hinton, G. E., Roweis, S. T., and Salakhutdinov, R. R. Neighbourhood components analysis. In Saul, L. K., Weiss, Y., and Bottou, L. (eds.), *Advances in Neural Information Processing Systems 17*, pp. 513–520. MIT Press, 2005.

Huber, P. J. A robust version of the probability ratio test. *Annals of Mathematical Statistics*, 36(6):1753–1758, 1965.

Kingma, D. P. and Ba, J. Adam: A method for stochastic optimization. *arXiv preprint arXiv:1412.6980*, 2014.

Koch, G., Zemel, R., and Salakhutdinov, R. Siamese neural networks for one-shot image recognition. In *ICML deep learning workshop*, volume 2. Lille, 2015.

Krizhevsky, A., Nair, V., and Hinton, G. Cifar-10 (canadian institute for advanced research). 2020.

Kuhn, D., Esfahani, P. M., Nguyen, V. A., and Shafieezadeh-Abadeh, S. Wasserstein distributionally robust optimization: Theory and applications in machine learning. In *Operations Research & Management Science in the Age of Analytics*, pp. 130–166. INFORMS, 2019.

Lake, B. M., Salakhutdinov, R., and Tenenbaum, J. B. Human-level concept learning through probabilistic program induction. *Science*, 350(6266):1332–1338, 2015.

LeCun, Y. and Cortes, C. MNIST handwritten digit database. 2010.

Lee, K., Maji, S., Ravichandran, A., and Soatto, S. Meta-learning with differentiable convex optimization. In *Proceedings of the IEEE Conference on Computer Vision and Pattern Recognition*, pp. 10657–10665, 2019.

Li, F., Fergus, R., and Perona, P. One-shot learning of object categories. *IEEE Transactions on Pattern Analysis and Machine Intelligence*, 28(4):594–611, 2006.

Plötz, T. and Roth, S. Neural nearest neighbors networks. In *Proceedings of the 32nd International Conference on Neural Information Processing Systems*, NIPS’18, pp. 1095–1106, Red Hook, NY, USA, 2018. Curran Associates Inc.

Salakhutdinov, R. and Hinton, G. Learning a nonlinear embedding by preserving class neighbourhood structure. In Meila, M. and Shen, X. (eds.), *Proceedings of the Eleventh International Conference on Artificial Intelligence and Statistics*, volume 2 of *Proceedings of Machine Learning Research*, pp. 412–419, San Juan, Puerto Rico, 21–24 Mar 2007. PMLR.

Samworth, R. J. et al. Optimal weighted nearest neighbour classifiers. *The Annals of Statistics*, 40(5):2733–2763, 2012.

Shafieezadeh-Abadeh, S., Kuhn, D., and Esfahani, P. M. Regularization via mass transportation. *Journal of Machine Learning Research*, 20(103):1–68, 2019.

Shalev-Shwartz, S. and Ben-David, S. *Understanding machine learning: From theory to algorithms*. Cambridge university press, 2014.

Shapiro, A., Dentcheva, D., and Ruszczyński, A. *Lectures on stochastic programming: modeling and theory*. SIAM, 2014.

Sinha, A., Namkoong, H., and Duchi, J. Certifying some distributional robustness with principled adversarial training. *arXiv preprint arXiv:1710.10571*, 2017.

Snell, J., Swersky, K., and Zemel, R. Prototypical networks for few-shot learning. In Guyon, I., Luxburg, U. V., Bengio, S., Wallach, H., Fergus, R., Vishwanathan, S., and Garnett, R. (eds.), *Advances in Neural Information Processing Systems 30*, pp. 4077–4087. Curran Associates, Inc., 2017.

Villani, C. *Optimal transport: old and new*, volume 338. Springer Science & Business Media, 2008.

Vinyals, O., Blundell, C., Lillicrap, T., Kavukcuoglu, K., and Wierstra, D. Matching networks for one shot learning. In *Proceedings of the 30th International Conference on Neural Information Processing Systems*, NIPS’16, pp. 3637–3645, Red Hook, NY, USA, 2016. Curran Associates Inc. ISBN 9781510838819.

Wang, Y., Yao, Q., Kwok, J., and Ni, L. M. Generalizing from a few examples: A survey on few-shot learning, 2019.

Yang, X., He, X., Zhao, J., Zhang, Y., Zhang, S., and Xie, P. COVID-CT-Dataset: A CT scan dataset about COVID-19, 2020.

Distributionally Robust Weighted k -Nearest Neighbors: Supplementary Materials

A. Proofs for Section 3

A.1. Proof of Theorem 1

The proof of Theorem 1 is based on the following two lemmas.

Lemma 1. *Fix probability distributions $P_1, \dots, P_M \in \mathcal{P}(\widehat{\Xi})$, where $\widehat{\Xi} = \{\xi^1, \dots, \xi^n\}$. Then*

$$\psi(P_1, \dots, P_M) := \min_{\pi: \widehat{\Xi} \rightarrow \Delta_M} \Psi(\pi; P_1, \dots, P_M) = M - \sum_{i=1}^n \max_{1 \leq m \leq M} P_m(\xi^i).$$

Furthermore, the optimal classifier π^* satisfies that for any $\xi^i \in \widehat{\Xi}$,

$$\{m : \pi_m^*(\xi^i) > 0, 1 \leq m \leq M\} \subset \arg \max_{1 \leq m \leq M} \frac{P_m(\xi^i)}{\sum_{m=1}^M P_m(\xi^i)}.$$

This lemma gives a closed-form expression for the risk of the optimal classifier if P_1, \dots, P_M are known, and shows that the optimal decision π^* accepts the class with the maximum likelihood. Moreover, when there is a tie (i.e., the set $\arg \max_{1 \leq m \leq M} P_m(\xi)$ is not singleton), the optimal decision π^* can break the tie arbitrarily.

Proof of Lemma 1. We here prove a more general result for an arbitrary sample space Ξ . Note that each $P_m, 1 \leq m \leq M$, is absolutely continuous with respect to $P_1 + \dots + P_M$, hence the Radon-Nikodym derivative $\frac{dP_m}{d(P_1 + \dots + P_M)}$ exists. Using the interchangeability principle (Shapiro et al., 2014) that enables us to exchange the minimization and integration, we have

$$\begin{aligned} \min_{\pi: \Xi \rightarrow \Delta_M} \Psi(\pi; P_1, \dots, P_M) &= \min_{\pi: \Xi \rightarrow \Delta_M} \int_{\Xi} \left[\sum_{m=1}^M (1 - \pi_m(\xi)) \frac{dP_m}{d(P_1 + \dots + P_M)}(\xi) \right] d(P_1 + \dots + P_M) \\ &= \int_{\Xi} \min_{\pi \in \Delta_M} \left[\sum_{m=1}^M (1 - \pi_m) \frac{dP_m}{d(P_1 + \dots + P_M)}(\xi) \right] d(P_1 + \dots + P_M) \\ &= \int_{\Xi} \left[1 - \max_{1 \leq m \leq M} \frac{dP_m}{d(P_1 + \dots + P_M)}(\xi) \right] d(P_1 + \dots + P_M), \end{aligned}$$

where the first equality is obtained by plugging in the definition of Ψ in (1); the second equality is due the interchangeability principle; and the last equality holds because for any ξ , the inner minimization attains its minimum at one of the vertices of Δ_M . If we substitute Ξ with the empirical support $\widehat{\Xi}$, the above formulation translates into

$$\min_{\pi: \widehat{\Xi} \rightarrow \Delta_M} \Psi(\pi; P_1, \dots, P_M) = M - \sum_{i=1}^n \max_{1 \leq m \leq M} P_m(\xi^i),$$

therefore the lemma is proved. \square

Lemma 2. *For the uncertainty sets defined in (7), the problem $\max_{P_m \in \mathcal{P}_m, 1 \leq m \leq M} \psi(P_1, \dots, P_M)$ is equivalent to (9).*

Proof of Lemma 2. Recall that the Wasserstein metric of order 1 is defined as

$$\mathcal{W}(P, P') := \min_{\gamma} \mathbb{E}_{(\xi, \xi') \sim \gamma} [c(\xi, \xi')]$$

for any two distributions P and P' on Ξ , where the minimization of γ is taken over the set of all probability distributions on $\Xi \times \Xi$ with marginals P and P' . By the definition of uncertainty sets in (7), we can introduce additional variables $\gamma_m \in \mathbb{R}_+^{n \times n}$ which represents the distribution on $\widehat{\Xi} \times \widehat{\Xi}$, with marginals $P_m \in \mathcal{P}_m$ and \widehat{P}_m , for $1 \leq m \leq M$. The constraints $\mathcal{W}(P, \widehat{P}_m) \leq \vartheta_m$ in (7) can be rewritten using γ_m as

$$\sum_{i=1}^n \sum_{j=1}^n \gamma_m^{i,j} c(\xi^i, \xi^j) \leq \vartheta_m, \quad m = 1, \dots, M.$$

Furthermore, the marginal distribution constraint of γ_m reads

$$\sum_{i=1}^n \gamma_m^{i,j} = \widehat{P}_m(\xi^j), \quad \sum_{j=1}^n \gamma_m^{i,j} = P_m(\xi^i), \quad m = 1, \dots, M.$$

Thereby the problem $\max_{P_m \in \mathcal{P}_m, 1 \leq m \leq M} \psi(P_1, \dots, P_M)$ is equivalent to the convex optimization formulation in (9). \square

Proof to Theorem 1. By Lemmas 1 and 2, we have

$$\max_{P_m \in \mathcal{P}_m, 1 \leq m \leq M} \min_{\pi: \widehat{\Xi} \rightarrow \Delta_M} \Psi(\pi; P_1, \dots, P_M) = \max_{P_m \in \mathcal{P}_m, 1 \leq m \leq M} \psi(P_1, \dots, P_M) = (9).$$

To prove Theorem 1, it remains to verify the validity of exchanging max and min. We identify π as (π^1, \dots, π^n) , where $\pi^i \in \mathbb{R}_+^M$ satisfies $\sum_{m=1}^M \pi_m^i = 1$. Similar to the proof of Lemma 2, P_m , $1 \leq m \leq M$, can also be identified as a vector in \mathbb{R}^n . Note that the objective function $\Psi(\pi; P_1, \dots, P_M)$ is linear in (π^1, \dots, π^n) and concave in (P_1, \dots, P_M) , and the Slater condition holds. Hence applying convex programming duality we can exchange max and min and thus the result follows. It is worth mentioning that the optimal solution π^* and corresponding LFDs P_1^*, \dots, P_M^* always exist since they are solutions to a saddle point problem. \square

A.2. Proof of Theorem 2

Proof of Theorem 2. On the one hand, since $\pi^{\text{knn}}(\cdot; k, w)$ can be regarded as a special case of the general classifier $\pi: \Xi \rightarrow \Delta_M$, it holds that

$$\begin{aligned} & \min_{\substack{w_m: \Xi \times \Xi \rightarrow \mathbb{R}_+, 1 \leq m \leq M \\ 1 \leq k \leq n}} \max_{P_m \in \mathcal{P}_m, 1 \leq m \leq M} \sum_{m=1}^M \mathbb{E}_{\xi_m \sim P_m} [1 - \pi_m^{\text{knn}}(\xi_m; k, w)] \\ & \geq \min_{\pi: \widehat{\Xi} \rightarrow \Delta_M} \max_{P_m \in \mathcal{P}_m, 1 \leq m \leq M} \sum_{m=1}^M \mathbb{E}_{\xi_m \sim P_m} [1 - \pi_m(\xi_m)]. \end{aligned}$$

On the other hand, by Lemma 2, there exists an optimal solution to the minimax problem (8), denoted as (P_1^*, \dots, P_M^*) , and the optimal classifier π^* as given in Lemma 1. Note that there exists $1 \leq k^* \leq n$ and weight functions w_1^*, \dots, w_M^* such that

$$\pi_m^{\text{knn}}(\xi; k^*, w^*) = \pi^*(\xi), \quad \forall \xi \in \widehat{\Xi}, \quad (13)$$

for example, by taking $k^* = 1$ and $w_m^* = P_m^*$, $1 \leq m \leq M$. This implies that

$$\begin{aligned} & \min_{\substack{w_m: \Xi \times \Xi \rightarrow \mathbb{R}_+, 1 \leq m \leq M \\ 1 \leq k \leq K}} \max_{P_m \in \mathcal{P}_m, 1 \leq m \leq M} \sum_{m=1}^M \mathbb{E}_{\xi_m \sim P_m} [1 - \pi_m^{\text{knn}}(\xi_m; k, w)] \\ & \leq \max_{P_m \in \mathcal{P}_m, 1 \leq m \leq M} \sum_{m=1}^M \mathbb{E}_{\xi_m \sim P_m} [1 - \pi_m^{\text{knn}}(\xi_m; k^*, w^*)] \\ & = \max_{P_m \in \mathcal{P}_m, 1 \leq m \leq M} \sum_{m=1}^M \mathbb{E}_{\xi_m \sim P_m} [1 - \pi_m^*(\xi_m)] \\ & = \min_{\pi: \widehat{\Xi} \rightarrow \Delta_M} \max_{P_m \in \mathcal{P}_m, 1 \leq m \leq M} \sum_{m=1}^M \mathbb{E}_{\xi_m \sim P_m} [1 - \pi_m(\xi_m)]. \end{aligned}$$

Thereby we have shown that formulations (6) and (8) have identical optimal values. Moreover, by the strong duality results in Theorem 1, we know $(\pi^*; P_1^*, \dots, P_M^*)$ is the saddle point for the formulation (8), and by the above arguments, we see that $(\pi^{\text{knn}}; P_1^*, \dots, P_M^*)$ leads to the same optimal value for formulation (6) as $(\pi^*; P_1^*, \dots, P_M^*)$ for formulation (8). Therefore, we show that π^{knn} is indeed the optimal solution to (6). \square

A.3. Proof of Theorem 3

Proof of Theorem 3. We now analyze the generalization error of the 1-NN classifier with the 0-1 loss. For completeness, we also review the classical results for the Bayes optimal test and the vanilla 1-NN rule.

Recall that Ξ is the feature space, $\mathcal{Y} = \{1, \dots, M\}$ is the label space, \mathcal{D} is a distribution over $\Xi \times \mathcal{Y}$, \mathcal{D}_Ξ is the marginal distribution of feature vectors ξ , and $\eta: \Xi \rightarrow \Delta_M$ is the conditional probability over the labels, i.e.,

$$\eta_m(\xi) = \mathbb{P}[y = m | \xi].$$

We assume that the conditional probability function η_m , for $1 \leq m \leq M$, is C -Lipschitz for some constant $C > 0$:

$$|\eta_m(\xi) - \eta_m(\xi')| \leq C \cdot c(\xi, \xi'), \quad \forall \xi, \xi' \in \Xi.$$

Intuitively, this assumption means that if two feature vectors are close to each other, then their labels are likely to be the same. The 0-1 loss function for a randomized test π is defined as

$$\ell(\pi, (\xi, y)) = 1 - \pi_y(\xi),$$

i.e., the probability that the correct class y is not accepted. Let

$$L_{\mathcal{D}}(\pi) = \mathbb{E}_{(\xi, y) \sim \mathcal{D}} [\ell(\pi, (\xi, y))]$$

be the population loss for randomized classifier π . Recall the Bayes optimal rule, i.e., the classifier that minimizes $L_{\mathcal{D}}(\pi)$ over all classifiers, is

$$\pi_m^*(\xi) = \begin{cases} 1 & m = \arg \max_{1 \leq m \leq M} \eta_m(\xi), \\ 0 & \text{otherwise,} \end{cases}$$

where the tie can be broken arbitrarily. More specifically, the Bayes optimal rule accept the class that enjoys the largest conditional probability. The error of the Bayes optimal classifier is

$$L_{\mathcal{D}}(\pi^*) = \mathbb{E}_{\xi \sim \mathcal{D}_\Xi} [1 - \max_{1 \leq m \leq M} \eta_m(\xi)].$$

Let π^S be the corresponding distributionally robust 1-NN classifier given i.i.d. samples $S = (\xi^1, y^1), \dots, (\xi^n, y^n)$. Then we have

$$\mathbb{E}_{S \sim \mathcal{D}^n} [L_{\mathcal{D}}(\pi^S)] = \mathbb{E}_{S_\xi \sim \mathcal{D}_\Xi^n, \xi \sim \mathcal{D}_\Xi, y \sim \eta(\xi)} [1 - \pi_y^S(\xi)],$$

where $S_\xi = (\xi^1, \dots, \xi^n)$ denotes the empirical features. For each query point ξ , its nearest neighbor is denoted as $\xi^{\tau_1^S(\xi)}$ and we have

$$p_m(\xi) = w_m(\xi, \xi^{\tau_1^S(\xi)}) = P_m^*(\xi^{\tau_1^S(\xi)}), \quad m = 1, \dots, M.$$

For any two feature vectors ξ and $\xi^{\tau_1^S(\xi)}$, we have from the law of total probability that

$$\mathbb{E}_{y \sim \eta(\xi)} [1 - \pi_y^S(\xi)] = \sum_{m=1}^M \mathbb{E}_{y \sim \eta(\xi)} [1 - \pi_y^S(\xi) | y^{\tau_1^S(\xi)} = m] \cdot \eta_m(\xi^{\tau_1^S(\xi)}).$$

As a baseline, we note that if there is no tie for the LFDs $\{P_1^*, \dots, P_M^*\}$, i.e., there is a unique class m such that $p_m(\xi) = P_m^*(\xi^{\tau_1^S(\xi)})$ is maximized, then this class m must equal to the label of the nearest neighbor $\xi^{\tau_1^S(\xi)}$ due to the definition of the empirical distributions and uncertainty sets in (7). Therefore, if there is no tie, the distributionally robust

weighted 1-NN classifier reduces to the vanilla 1-NN, and we determine the class for ξ the same as the class of its nearest neighbor $\xi^{\tau_1^S(\xi)}$, thus we have $\pi_y^S(\xi) = m$ and

$$\begin{aligned}
 & \mathbb{E}_{y \sim \eta(\xi), y^{\tau_1^S(\xi)} \sim \eta(\xi^{\tau_1^S(\xi)})} [1 - \pi_y^S(\xi)] \\
 &= \sum_{m=1}^M (1 - \eta_m(\xi)) \cdot \eta_m(\xi^{\tau_1^S(\xi)}) \\
 &= \sum_{m=1}^M (1 - \eta_m(\xi)) \cdot (\eta_m(\xi^{\tau_1^S(\xi)}) - \eta_m(\xi) + \eta_m(\xi)) \\
 &= \sum_{m=1}^M (1 - \eta_m(\xi)) \cdot \eta_m(\xi) + \sum_{m=1}^M (1 - \eta_m(\xi)) \cdot (\eta_m(\xi^{\tau_1^S(\xi)}) - \eta_m(\xi)) \\
 &\leq \sum_{m=1}^M (1 - \eta_m(\xi)) \cdot \eta_m(\xi) + \sum_{m=1}^M (1 - \eta_m(\xi)) \cdot C \cdot c(\xi, \xi^{\tau_1^S(\xi)}) \\
 &= \sum_{m=1}^M (1 - \eta_m(\xi)) \cdot \eta_m(\xi) + (M-1)C \cdot c(\xi, \xi^{\tau_1^S(\xi)}).
 \end{aligned} \tag{14}$$

Note that we have

$$\sum_{m=1}^M (1 - \eta_m(\xi)) \cdot \eta_m(\xi) \leq M(1 - \max_{1 \leq m \leq M} \eta_m(\xi)),$$

substitute into (14), we conclude that if there is no tie for the LFDs on the empirical samples, we have

$$\mathbb{E}_{S \sim \mathcal{D}^n} [L_{\mathcal{D}}(\pi^S)] \leq M L_{\mathcal{D}}(\pi^*) + (M-1)C \cdot \mathbb{E}_{S, \xi} [c(\xi, \xi^{\tau_1^S(\xi)})]. \tag{15}$$

The second term can be bounded using Theorem 19.3 in (Shalev-Shwartz & Ben-David, 2014).

Now we analyze the risk bound for the distributionally robust 1-NN classifier when there is a tie. More specifically, the tie means that the LFDs at the point $\xi^{\tau_1^S(\xi)}$ does not have a unique maximum. Recall that for given samples S , we assume there is a tie at $\xi^{\tau_1^S(\xi)}$ between classes $m_1^S, \dots, m_{K_S}^S$ for some $K_S \leq M$. Note that there exist $1 \leq i \leq K_S$ such that $m_i = y^{\tau_1^S(\xi)}$, i.e., the class of the nearest neighbor $\xi^{\tau_1^S(\xi)}$ should be within the tied classes. Recall we accept class m_k^S with probability $\pi_{m_k^S}^S(\xi)$, for $0 \leq \pi_{m_k^S}^S(\xi) \leq 1$ and $\sum_{k=1}^{K_S} \pi_{m_k^S}^S(\xi) = 1$. Note that π^S here corresponds to the randomized test π^{knn} that corresponds to the optimal solution to (6).

The corresponding risk is

$$\mathbb{E}_{y \sim \eta(\xi)} [1 - \pi_y^S(\xi)] = \sum_{k=1}^{K_S} \pi_{m_k^S}^S(\xi) \cdot (1 - \eta_{m_k^S}(\xi)). \tag{16}$$

Compared with the case when there is no tie (14), we have the difference reads

$$\begin{aligned}
 (16) - (14) &= \sum_{k=1}^{K_S} \pi_{m_k^S}^S(\xi) \cdot (1 - \eta_{m_k^S}(\xi)) - \sum_{m=1}^M (1 - \eta_m(\xi)) \cdot \eta_m(\xi^{\tau_1^S(\xi)}) \\
 &= \sum_{m=1}^M \left(\sum_{k=1}^{K_S} \pi_{m_k^S}^S(\xi) (1 - \eta_{m_k^S}(\xi)) - (1 - \eta_m(\xi)) \right) \cdot \eta_m(\xi^{\tau_1^S(\xi)}), \\
 &= \sum_{m=1}^M \left(\eta_m(\xi) - \sum_{k=1}^{K_S} \pi_{m_k^S}^S(\xi) \eta_{m_k^S}(\xi) \right) \cdot \eta_m(\xi^{\tau_1^S(\xi)})
 \end{aligned}$$

which means that for a particular feature value $\xi \in \Xi$, the risk in (16) is smaller than the risk in (14) when we have

$$\sum_{m=1}^M \left(\eta_m(\xi) - \sum_{k=1}^{K_S} \pi_{m_k^S}^S(\xi) \eta_{m_k^S}(\xi) \right) \cdot \eta_m(\xi^{\tau_1^S(\xi)}) < 0, \tag{17}$$

which can be viewed as the weighted average over

$$\eta_m(\xi) = \sum_{k=1}^{K_S} \pi_{m_k^S}^S(\xi) \eta_{m_k^S}(\xi),$$

with the weights being $\eta_m(\xi^{\tau_1^S(\xi)})$, $1 \leq m \leq M$.

Note that the risk formulation in (16) is general and will be reduced to the no-tie case when we have $K_S = 1$ and thus $\pi_m^S(\xi) = 1$ for m equal the label of $\xi^{\tau_1^S(\xi)}$. The population risk of the distributionally robust weighted k -NN classifier can be computed by taking expectation with respect to the sample $S \sim \mathcal{D}^n$ of (16). \square

B. Memory-efficient implementation of Dr. k-NN in data-intensive scenario

For the sake of completeness, we extend our algorithm to non-few-training-sample setting. This can be particularly useful for the general classification problem with an arbitrary size of training set. In fact, k -NN methods notoriously suffer from computational inefficiency if the number of labeled samples n is large, since it has to store and search through the entire training set (Goldberger et al., 2005).

The main idea is to only keep the training samples that are important in deciding the decision boundary based on the maximum entropy principle (Cover & Thomas, 2006). As a measure of importance, we choose the samples with the largest entropy across all categories, based on the intuition that the samples with higher entropy has larger uncertainty and will be more useful for classification purposes since they tend to lie on the decision boundary. The entropy of a sample is defined as follows. Consider a random variable which takes value m with probability π_m , $\sum_{m=1}^M \pi_m = 1$; then the entropy of this random variable is defined as

$$H(\pi_1, \dots, \pi_M) = - \sum_{m=1}^M \pi_m \log \pi_m.$$

As a simple example, for Bernoulli random variable (which can represent, e.g., the outcome for flipping a coin with bias p), the entropy function is $H(p) = -p \log p - (1-p) \log(1-p)$, and it is a concave function achieving the maximum at $p^* = 1/2$, which means that the fair-coin has the maximum entropy; this is intuitive as indeed the outcome of a fair coin toss is the most difficult to predict. Now we use this entropy to define the “uncertainty” associated with each training points. With a little abuse of notation, define

$$H(\hat{\xi}) := H(\pi_1(\hat{\xi}), \dots, \pi_M(\hat{\xi})).$$

Denote the minimal and maximal entropy of all the training points as

$$H_{\min} = \min\{H(\hat{\xi}), \hat{\xi} \in \hat{\Xi}\}, \quad H_{\max} = \max\{H(\hat{\xi}), \hat{\xi} \in \hat{\Xi}\}.$$

Define the τ -truncated training set as

$$\tilde{\Xi} = \{\hat{\xi} \in \hat{\Xi} : (H(\hat{\xi}) - H_{\min}) / (H_{\max} - H_{\min}) \geq \tau\}, \forall \tau \in [0, 1].$$

The truncated Dr. k-NN is obtained similarly as Step 2 of Dr. k-NN by restricting the training set $\tilde{\Xi}$ only to the samples in $\tilde{\Xi}$ (samples with larger entropy). Figure 5 reveals that the most informative samples usually lie in between categories. We can see that a truncated Dr. k-NN classifier with $\tau = 0.9$ only uses 20% samples with little performance loss. More experimental details is presented in Section 5.

C. Comparison to kernel smoothing

Figure 8 and Figure 9 present a comparison of the results using $\text{Dr. } k\text{-NN}$ and the kernel smoothing defined in (12). The results suggest that the performance of $\text{Dr. } k\text{-NN}$ is insensitive to the choice of k , while the performance of the kernel smoothing is heavily depended on the choice of h .

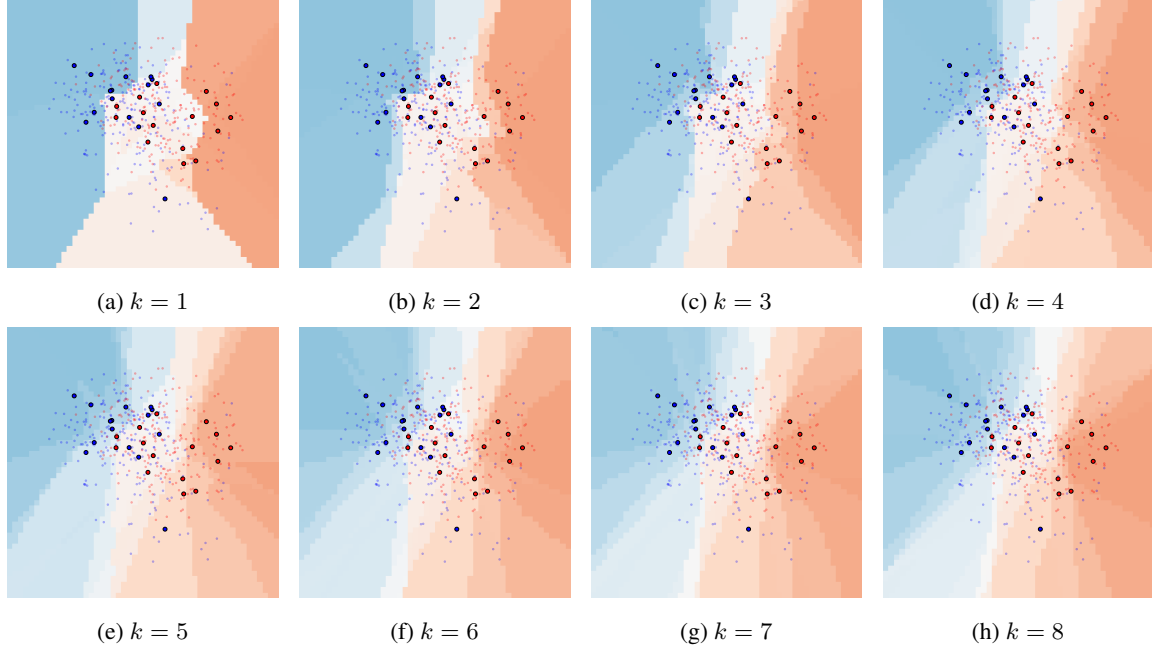


Figure 8. $\text{Dr. } k\text{-NN}$ with different k .

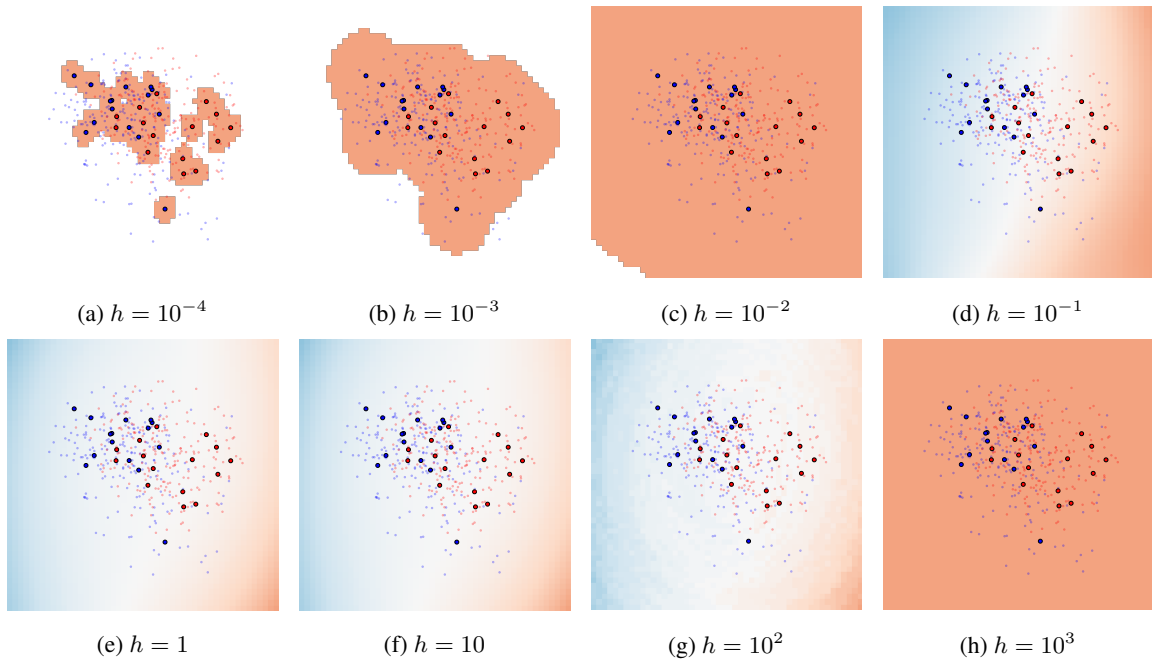


Figure 9. Kernel smoothing with different bandwidth h .

D. Real data examples for COVID-19 CT

Figure 10 and Figure 11 show 16 real CT images collected from patients who have been diagnosed with COVID-19 and other diseases (non-COVID-19), respectively.

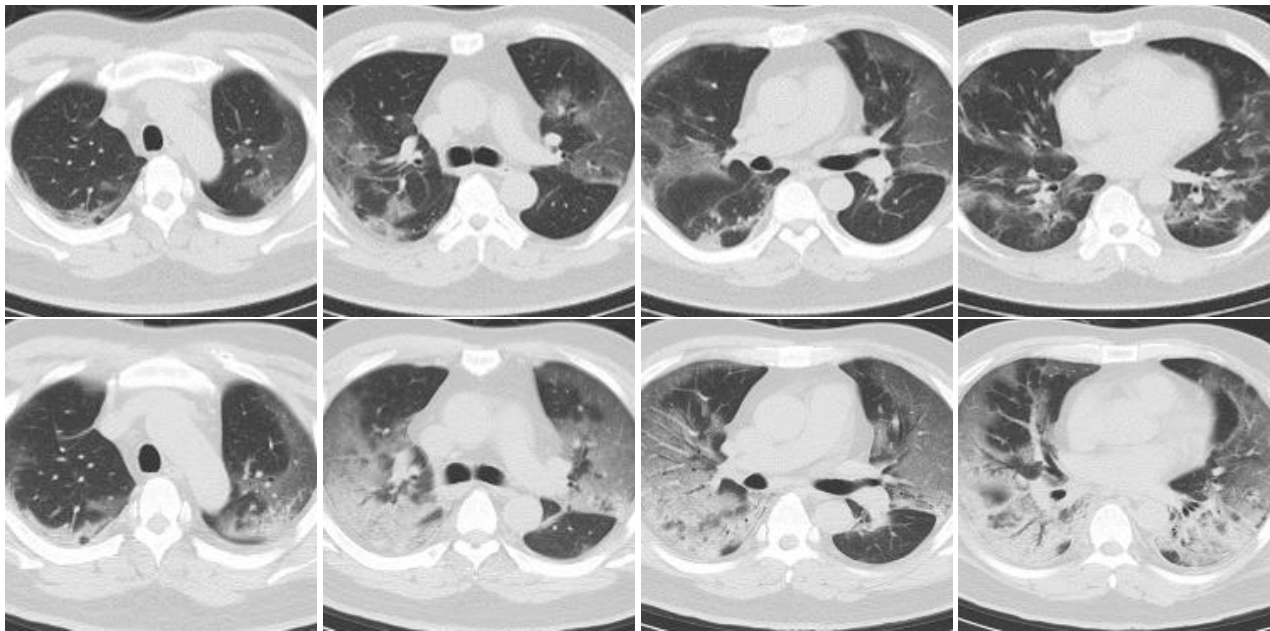


Figure 10. COVID-19 CT images.

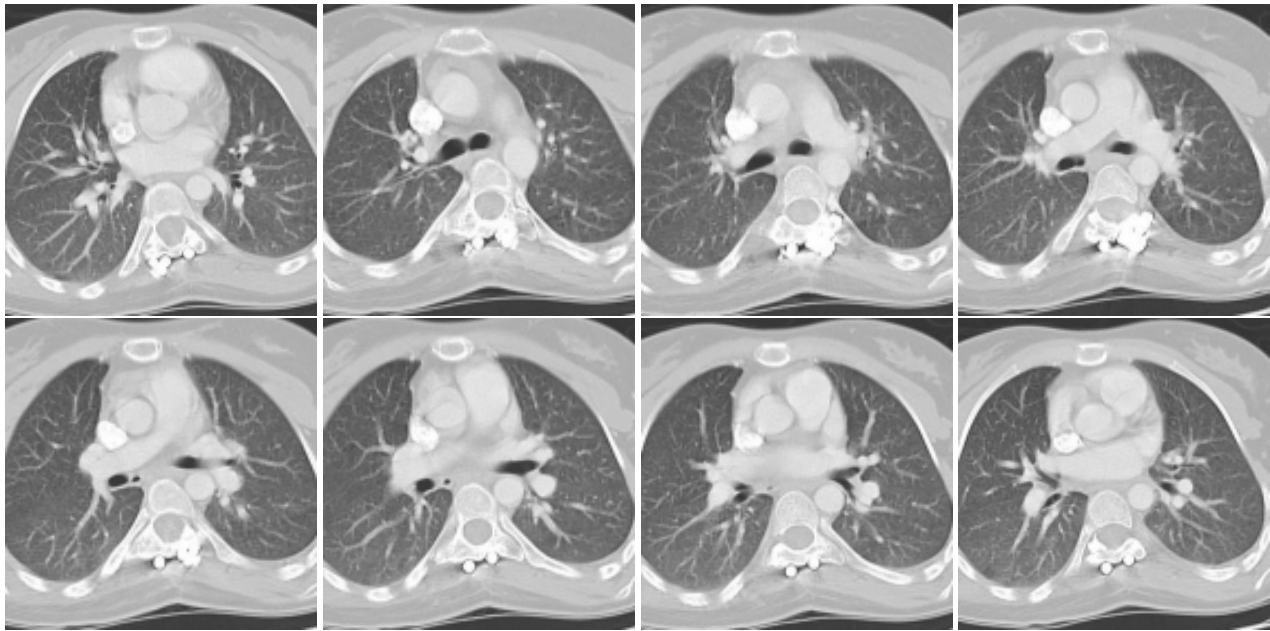


Figure 11. Non-COVID-19 CT images.